

Characterization and Cloning of an Extremely Thermostable, *Pyrococcus furiosus*-Type 4Fe Ferredoxin from *Thermococcus profundus*

Takeo Imai,^{*1} Katsuhiko Taguchi,^{*} Yoko Ogawara,^{*} Daijiro Ohmori,[†] Fumiya Yamakura,[†] Hidenori Ikezawa,[‡] and Akio Urushiyama^{*}

^{*}Department of Chemistry, College of Science, Rikkyo (St Paul's) University, Toshima-ku, Tokyo 171-8501,

[†]Department of Chemistry, Juntendo University, School of Medicine, Inba, Chiba 270-1695, and [‡]ThermoQuest Co., Shibuya, Tokyo 151-0061

Received June 12, 2001; accepted August 27, 2001

An extremely thermostable [4Fe-4S] ferredoxin was isolated under anaerobic conditions from a hyperthermophilic archaeon *Thermococcus profundus*, and the ferredoxin gene was cloned and sequenced. The nucleotide sequence of the ferredoxin gene shows the ferredoxin to comprise 62 amino acid residues with a sequence similar to those of many bacterial and archaeal 4Fe (3Fe) ferredoxins. The unusual Fe-S cluster type, which was identified in the resonance Raman and EPR spectra, has three cysteines and one aspartate as the cluster ligands, as in the *Pyrococcus furiosus* 4Fe ferredoxin. Under aerobic conditions, a ferredoxin was purified that contains a [3Fe-4S] cluster as the major Fe-S cluster and a small amount of the [4Fe-4S] cluster. Its N-terminal amino acid sequence is the same as that of the anaerobically-purified ferredoxin up to the 26th residue. These results indicate that the 4Fe ferredoxin was degraded to 3Fe ferredoxin during aerobic purification. The aerobically-purified ferredoxin was reversibly converted back to the [4Fe-4S] ferredoxin by the addition of ferrous ions under reducing conditions. The anaerobically-purified [4Fe-4S] ferredoxin is quite stable; little degradation was observed over 20 h at 100°C, while the half-life of the aerobically-purified ferredoxin is 10 h at 100°C. Both the anaerobically- and aerobically-purified ferredoxins were found to function as electron acceptors for the pyruvate-ferredoxin oxidoreductase purified from the same archaeon.

Key words: 4Fe ferredoxin, interconversion, non-cysteinylligand, *Thermococcus profundus*, thermostable.

The three-dimensional structure of the [4Fe-4S] ferredoxin from *Bacillus thermoproteolyticus* has been analyzed by X-ray crystallography by Fukuyama *et al.* (1, 2). After their analysis, the structures of mesophilic *Desulfovibrio gigas* [3Fe-4S] ferredoxin (3), *D. africanus* ferredoxin I (4) and hyperthermophilic [4Fe-4S] ferredoxin derived from *Thermotoga maritima* (5) were characterized by the same technique. Recently, the structure of the [4Fe-4S] ferredoxin from *Pyrococcus furiosus* was solved by X-ray crystallographic analysis as a cocrystal with formaldehyde-ferredoxin oxidoreductase isolated from the same bacterium (6). These X-ray crystallographic analyses revealed that all the above 4Fe (3Fe) ferredoxins are quite similar to each other in three-dimensions. Many 4Fe and 3Fe ferredoxins have also been found to have similar primary structures to those of the ferredoxins described above (7). In addition, almost all 4Fe and 3Fe ferredoxins contain the Fe-S cluster-binding motif, CXXCXXCXXXCP, in the N-terminal region. In the case of these 4Fe ferredoxins, the first three cysteine residues in the motif and another cysteine residue in the

C-terminal half are the ligands that coordinate the [4Fe-4S] cluster (1–5).

In contrast to the ferredoxins described above, a 4Fe ferredoxin from *P. furiosus* has been shown to have an anomalous coordination constructed by an aspartic acid residue-containing Fe-S cluster binding motif, C¹¹XXDXX-CXXXCP²², in the N-terminal region and also a cysteine residue in the C-terminal half (9). This has subsequently been confirmed by ¹H-NMR spectroscopy (8) and X-ray crystallography (6). This latter ferredoxin exhibits several abnormal physicochemical properties as observed in the EPR, resonance Raman, and low temperature MCD spectra due to the unusual aspartic acid ligand (9).

The hyperthermophilic archaeon *Thermococcus profundus*, which was isolated from a deep-sea hydrothermal vent system in the Middle Okinawa Trough in Japan, grows optimally at 80°C at pH 7–7.5 on tryptone and inorganic sulfur, and produces H₂S during growth (10). Here we report the characterization, amino acid sequence, thermal stability, and biological function of the *T. profundus* [4Fe-4S] ferredoxin, which is the second instance in which a 4Fe ferredoxin contains an anomalous aspartic acid coordination binding motif. Several properties of the Fe-S cluster, including the interconversion between [4Fe-4S] and [3Fe-4S] clusters, are presented and discussed.

¹ To whom correspondence should be addressed. Phone/Fax: +81-3-3985-2372, E-mail: imaitak@rikkyo.ne.jp

MATERIALS AND METHODS

Materials—Bactotryptone and yeast extracts were obtained from the Difco Laboratories. Inorganic sulfur powder was purchased from Wako Co. Q Sepharose FF was obtained from Pharmacia Biotech. DEAE-TOYOPEARL and TOYOPEARL HW65C were purchased from TOSO. All other chemicals were of analytical grade.

Strain and Growth—*Thermococcus profundus* DSM DT5432 was grown on tryptone and yeast extract with inorganic sulfur and sodium sulfide in a medium described earlier (10).

Purification of Ferredoxins—Anaerobic purification was carried out as follows. Unless otherwise stated, all buffers were made anaerobic by degassing under reduced pressure followed by concomitant bubbling with purified Ar gas. This degassing-bubbling was repeated three times and then DTT and sodium dithionite were added to the degassed buffers at a concentration of 2 mM each. Ar gas was purified with a heated copper wire. All operations were performed anaerobically at ambient temperature (~25°C) mainly in an anaerobic chamber (Coy Laboratory). Unless otherwise indicated, the anaerobic buffer used was 50 mM Tris-HCl, pH 8.0/2 mM DTT/2 mM sodium dithionite.

Frozen *T. profundus* cells were thawed in the above buffer containing 10 mM sodium dithionite. The suspension was stirred overnight with pancreatic DNase I (1 mg)/RNase A (1 mg)/10 mM MgSO₄/buffer. The homogenate was centrifuged at 80,000 ×g for 40 min and the supernatant (cell-free extract) obtained was loaded onto a Q Sepharose FF column equilibrated with the buffer. The following chromatographic procedures with Q-Sepharose, DEAE-TOYOPEARL, and hydroxyapatite were essentially the same as in ref. 19 except that all buffers and the atmosphere were made anaerobic as described above. The purified ferredoxin was stored at -30°C under anaerobic conditions until use.

Aerobic purification was performed under atmospheric air by the same procedure as for anaerobic purification except that dithionite and DTT in the buffer were omitted. After purification, the ferredoxin solution was made anaerobic by standing for at least 14 h at ambient temperature in the presence of 2 mM DTT.

Analytical Procedures—The molecular weight of *T. profundus* ferredoxin was determined by two methods, amino acid sequence deduced from the corresponding nucleotide sequence of the ferredoxin gene and electrospray mass spectrum (see below). SDS-PAGE was performed by the literature method (11) with the exception that the ferredoxin sample was denatured at 121°C for 60 min in 1% SDS/1% mercaptoethanol. Native 30% PAGE was carried out by the method of Davis (12). Absorption spectra were recorded on a Nihonbunko model 530 UV-visible spectrophotometer using reducing reagent-free ferredoxin prepared by passing the ferredoxin solution through a small Sephadex G-25 column equilibrated with reducing reagent-free anaerobic 50 mM Tris-HCl, pH 8.0. The protein concentration was estimated by the method of Lowry *et al.* (13) after the apoprotein was precipitated by treatment with 5% trichloroacetic acid. Iron was determined by the *o*-phenanthroline method (14) using the supernatant obtained by trichloroacetic acid precipitation. Acid-labile sulfides were estimated by the methylene blue formation method (15). The N-terminal

amino acid sequence was determined by automatic protein sequencing; ferredoxin preparations (100 pmol) dialyzed overnight against water were transferred directly to a model 492 Precise Protein Sequencing System (ABI). The thermal stability of *T. profundus* ferredoxin (in 50 mM Tris-HCl, pH 8.0/2 mM DTT) was determined under anaerobic conditions by following the absorbance change at 440 nm during incubation at 100°C.

Cloning and Sequence Analysis of the Ferredoxin Gene from *T. profundus*—The two mixed oligonucleotides used to amplify the partial ferredoxin gene from *T. profundus* by PCR were synthesized on the basis of the N-terminal sequence of *T. profundus* ferredoxin (Trp²-Lys-Val-Thr-Val-Asp-Gln⁸, 5'GGCTGCAGTGGAAAGT-NACNGTNGAYCA-3') (this study) and the C-terminal sequence of *P. furiosus* ferredoxin (Cys⁴⁸-Ala-Lys-Glu-Ala-Met-Glu⁶⁴ 5'GGGAATTCTCCATNGCYTCYTTCGCRCA3') (R=A+G, N=A+G+C+T, Y=C+T) (16). The PCR-amplified fragments were cloned into pUC119. These cloned fragments were labeled with digoxigenin (Boehringer Mannheim Yamanouchi, Tokyo) and used as probes for the cloning. The probe was subjected to Southern hybridization analysis with only one chromosomal DNA fragment in the digest pattern. The fraction of the 2.3 kb *Sac*I-digested fragments that hybridized with the probe was isolated from an agarose gel, and these fragments were cloned into *Sac*I-digested pBluescript SK+ vector. The one clone that hybridized with this probe was identified in a DNA library of the strain.

Nucleotides were sequenced by the dideoxynucleotide chain termination method with an automated sequencer (model 373A; Applied Biosystems, Foster City, CA). Both DNA strands were sequenced by this method. The sequence reported in this study has been deposited in the DDBJ database (accession number AB042645).

Spectral Measurement—The purified *T. profundus* ferredoxin in anaerobic-dithionite-free 1 mM ammonium acetate/0.1 mM DTT was used for electrospray mass spectral measurements. The mass spectra were measured with a ThermoQuest LCQ model mass spectrometer. EPR spectra were recorded as described previously (17). The buffer of the purified ferredoxin was exchanged for the anaerobic reducing reagent-free buffer by centrifugation through a Microcon YM3 membrane (Amicon). The concentration of the ferredoxin was 2.5 mg/ml. Chemical reduction of the ferredoxin was carried out under an anaerobic atmosphere for 20 min in the presence of an aliquot of 0.5 M sodium dithionite/1 M Tris-HCl, pH 8.0, at a final concentration of 5 mM. Resonance Raman spectra were recorded with Ar⁺ laser excitation at 457.9 nm as described previously (18). The concentration of the ferredoxin was 5–8 mM. Five or ten molar excess ferricyanide-treated ferredoxin was prepared as described earlier (19) and the conversion of the [3Fe-4S] to [4Fe-4S] cluster was carried out by incubating 0.5 mM [3Fe-4S] ferredoxin with 1 mM FeSO₄/10 mM Tris-HCl, pH 8.0/2 mM sodium dithionite/2 mM DTT for 2 h at 25°C. The excess FeSO₄ in the reaction mixture was removed by Microcon 3 (Amicon).

Enzyme Assay and Enzyme—The biological activity of *T. profundus* ferredoxin was investigated in *T. profundus* pyruvate-ferredoxin oxidoreductase (20) in which methylviologen was replaced with anaerobic *T. profundus* ferredoxins. The UV-visible absorption spectra were measured in anaerobic 50 mM EPPS-Na buffer (pH 8.4)/2 mM DTT.

After the addition of *T. profundus* pyruvate-ferredoxin oxidoreductase (0.02 unit)/5 mM sodium pyruvate/1 mM magnesium sulfate/1 mM thiamine pyrophosphate/0.5 mM CoASH/(0.5 mM EDTA in some cases), the absorbance decrease at 440 nm was monitored at 80°C. After the absorbance decrease was completed, the spectrum was measured again after cooling the sample to ambient temperature. The pyruvate-ferredoxin oxidoreductase was purified from *T. profundus* cells with specific activities of 4.8–28.0 units/mg protein at 80°C. The enzyme was purified to homogeneity as determined by both native- and SDS-PAGE (unpublished observations).

RESULTS AND DISCUSSION

Purity of the Protein—The purity of the ferredoxin purified anaerobically or aerobically from *T. profundus* cells was examined by both 30% native- and 20% SDS-PAGE. Each purified sample gave a single band on both gels, suggesting that both ferredoxins were purified to homogeneity.

Nucleotide Sequence of the *T. profundus* Ferredoxin Gene and Its Corresponding Amino Acid Sequence—A total of 2,321 bp *Sac*I fragments, including the *T. profundus* ferredoxin gene, were sequenced. The sequence of a 400 bp region of *T. profundus* genomic DNA including the ferredoxin gene has been deposited in the DDBJ database: AB042645. A putative ribosome binding site (GATG, position -8 to -5) and an archaeal consensus promoter, Box A (TTTATATT, position -40 to -33), were identified upstream of the initiation site. Long stretches of pyrimidine-rich sequences, an archaeal transcription termination signal, were located downstream of the stop codon.

The primary sequence of the *T. profundus* ferredoxin (Fig. 1) was deduced from the nucleotide sequence and was found to correspond to the N-terminal 27 residues of the anaerobically-purified ferredoxin and also to the N-terminal 26 residues of the aerobically-purified ferredoxin determined by protein sequencing. *T. profundus* ferredoxin was found to comprise 62 amino acid residues and to exhibit high homology (expressed as “identity” calculated from the number of identical amino acids) with the *Pyrococcus kodakaraensis* 4Fe ferredoxin (92%) (21), *P. furiosus* 4Fe ferredoxin (74%) (16), *T. litoralis* 4Fe ferredoxin (69%) (16), *Ta. maritima* 4Fe ferredoxin (58%) (22, 23), *D. gigas* ferredoxin (40%) (24), *D. africanus* ferredoxin I (4Fe ferredoxin) (34%) (25) and *B. thermoproteolyticus* 4Fe ferredoxin (20%) (1). On the basis of sequence similarity, *T. profundus* ferredoxin can be thought to have a three-dimensional structure similar to that of *B. thermoproteolyticus* 4Fe ferredoxin (1, 2), as well as analogous ferredoxins (3–6). *T. profundus* ferredoxin also can be thought to have a disulfide bridge constructed by two cysteine residues at positions 21 and 44 (3, 26). The

molecular weight of *T. profundus* apoferreredoxin was calculated to be 6,450 from the amino acid sequence (Fig. 1). On the other hand, a value of 6,801 for the anaerobically-purified ferredoxin was obtained from the electrospray mass spectrum; the molecular weight difference (6,801–6,450 = 351) can be attributed to that of a single [4Fe-4S] cluster.

Fe-S Cluster—The presence of a [4Fe-4S] cluster in the anaerobically-purified *T. profundus* ferredoxin was confirmed by quantitative analyses of both iron (4.1 ± 0.2 mol/6,801 Da) and acid-labile sulfide (4.2 ± 0.3 mol/6,801 Da). The UV-visible absorption spectra of the anaerobically- and aerobically-purified ferredoxins are shown in Fig. 2. The spectrum of the former ferredoxin is typical to [4Fe-4S] cluster-containing ferredoxins with a peak at 280 nm and a shoulder at around 390 nm; the molar extinction coefficient at 390 nm is 16,500. The aerobically-purified ferredoxin exhibits peaks at 280 and 410 nm and its molar extinction coefficient is 18,900 mol⁻¹·cm⁻¹ at 410 nm. Subsequently, EPR and resonance Raman spectra were recorded to identify the Fe-S clusters in both ferredoxins. The EPR spectrum of anaerobically-purified ferredoxin is shown in Fig. 3a. The spectrum elicits signals around *g* = 2 and *g* = 5. The relative intensity of the signals increased ca. 10-fold by incubating the ferredoxin with sodium dithionite, and a broad signal at *g* = 2.6 appeared (Fig. 3b). The spectrum is composed of rhombic EPR signals at *g* = 2.13, 1.87, 1.81 attributable to the reduced *S* = 1/2 [4Fe-4S]⁺ cluster, and low field resonance around *g* = 5 (*g* = 5.54 and *g* = 4.93) with a broad signal at *g* = 2.64, which can be attributed to the *S* = 3/2 spin system (9). On the other hand, the aerobically-purified ferredoxin shows a signal at *g* = 2.01, typical of the [3Fe-4S]⁺ cluster (Fig. 3c). The resonance Raman spectrum of the anaerobically-purified *T. profundus* ferredoxin recorded

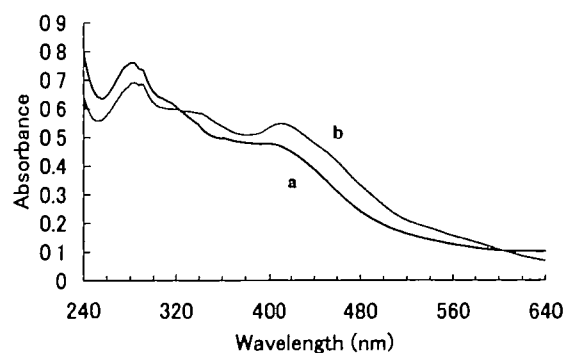


Fig 2 UV-visible absorption spectra of *T. profundus* ferredoxins. (a) Anaerobically-purified ferredoxin (b) Aerobically-purified ferredoxin. The concentration of both ferredoxins is 0.20 mg/ml in anaerobic 50 mM Tris-HCl, pH 8.0/0.2 M NaCl without DTT or sodium dithionite

Fig. 1. The amino acid sequence of *T. profundus* ferredoxin as well as other 4Fe (3Fe) ferredoxins isolated from bacteria and archaea. Open triangles show cysteine or aspartate ligands of the Fe-S cluster and closed triangles indicate cysteine residues that could form disulfide bridges. The asterisks (*) indicate common amino acid residues among the seven ferredoxins listed. Tp, *Thermococcus profundus*; Pk, *Pyrococcus kodakaraensis* KOD1; Pf, *Pyrococcus furiosus*; Tl, *Thermococcus litoralis*; Tm, *Thermotoga maritima*; Dg, *Desulfobubrio gigas*; Da, *Desulfobubrio africanus* (ferredoxin I).

		10	20	30	40	50	60
Tp	AWKVTVDQQT	CIGDAICASLCPDVFEMGDDG	-KAHPVDIT	D--LE-CAQEAAEAC	PVGAITL	EEA	
Pk	AWRVSDVDTC	CIGDAICASLCPDVFEMGDDG	-KAHPVVETT	D--LD-CAQEAAEAC	PVGAITL	EEA	
Pf	AWRVSDQQT	CIGDAICASLCPDVFEMNDEG	-KAQPKVEVI	EDEELYNCAKEAMEAC	PVGAITL	EEA	
Tl	-MKVSDKDAC	ICGCVGASICPDVFEMDDG	-KAKALVAET	D--LE-CAKEAAEAC	PTGAI	TVE	
Tm	-MKVRVDADAC	ICGCVENLCPDVFQLGDDG	-KAKVLQPET	D--LP-CAKDAADS	CPGAI	SVEE	
Dg	MP-IEVN-DDC	MACEACVEICPDVFEMNEEG	KAVVINPDS	D--LD-CVEEAI	DSCPAEAI	-IRS	
Da	ARKFYVDQDE	CAECSCVELAPGAFAMDPEIEKAYVKD	VEG-A--SQEVEVEA	HDTC	CPVQCI	HWED	

with 457.9 nm Ar⁺ laser excitation exhibits distinct bands at 252, 270, 283, 313, 342, 365, 376, and 393 cm⁻¹ (Fig. 4a). The spectrum closely resembles that of *P. furiosus* 4Fe ferredoxin (9). The aerobically-purified ferredoxin shows resonance Raman bands at 265, 290, 347, 360, 368, 385 cm⁻¹ (Fig. 4c), resembling those of 3Fe ferredoxins and 3Fe cluster-containing proteins with three cysteine residues as the cluster ligands.

In most 4Fe ferredoxins, the ligands of the [4Fe-4S] cluster are four cysteine residues (7), whereas one of the four cysteine ligands is replaced by an aspartate in *P. furiosus* 4Fe ferredoxin (8). The presence of the same Fe-S binding motif was suggested for *P. kodakaraensis* 4Fe ferredoxin (21). The sequence similarity of the *T. profundus* 4Fe ferredoxin to many archaeal and bacterial ferredoxins, as well as the presence of the motif CXXDXXCXXXCP in the N-terminal region (Fig. 1), suggests that the ligands of the [4Fe-4S] cluster are the three cysteines at positions 11, 17, and 52 and the aspartate at position 14 in *T. profundus* ferredoxin. This was confirmed by the resonance Raman spectrum shown in Fig. 4a; the ferredoxin exhibits a totally symmetric Fe-S stretching band at 342 cm⁻¹, similar to the case of *P. furiosus* ferredoxin (9). A corresponding band has been observed at 333–338 cm⁻¹ for normal [4Fe-4S] clusters with four cysteine residues as ligands (27). The abnormal EPR spectrum shown in Fig. 3b also indicates the presence of the unusual [4Fe-4S] cluster (9).

Oxygen Sensitivity and Fe-S Cluster Interconversion—It is well known that ferricyanide causes oxidative degradation of the [4Fe-4S] cluster to a [3Fe-4S] cluster. Therefore, ferricyanide-treated 4Fe ferredoxin has often been used as

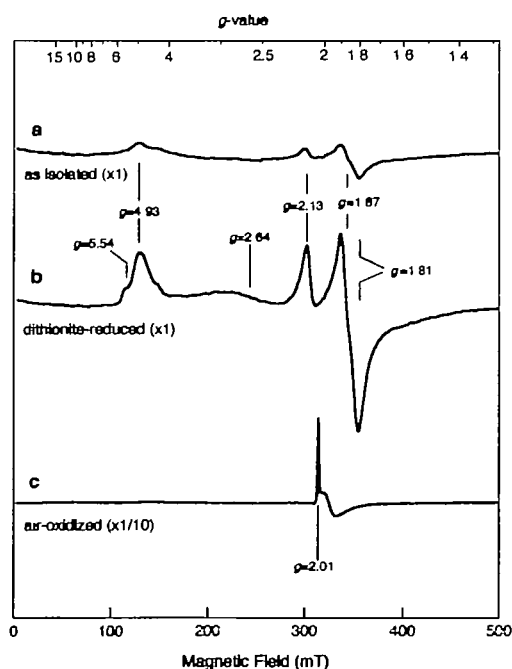


Fig 3 Low temperature EPR spectra of *T. profundus* ferredoxins. (a) Anaerobically-purified ferredoxin; (b) Excess dithionite-reduced anaerobically-purified ferredoxin; (c) Aerobically-purified ferredoxin. The ferredoxin concentrations were 2.5 mg/ml in 50 mM Tris-HCl, pH 8.0/0.2 M NaCl. Instrument settings: temperature, 8 K, modulation amplitude, 0.6 mT; microwave power, 5 mW. The *g*-values are indicated

a standard for the 3Fe ferredoxin. The resonance Raman spectrum of the *T. profundus* 4Fe ferredoxin treated with a five-fold molar excess of ferricyanide is shown in Fig. 4b. Treatment with a ten-fold molar excess of ferricyanide produced a similar spectrum. The spectrum is similar to the spectra of many [3Fe-4S] cluster-containing proteins, indicating that *T. profundus* 4Fe ferredoxin degrades into a 3Fe ferredoxin by ferricyanide treatment.

The resonance Raman spectrum of the aerobically-purified *T. profundus* ferredoxin is shown in Fig. 4c. This spectrum is not much different from the spectrum of the ferricyanide-treated sample (Fig. 4b). However, the difference spectrum (Fig. 4, c minus b) shown in Fig. 4d exhibits features characteristic of the anaerobically-purified ferredoxin. These results indicate that a large portion of *T. profundus* 4Fe ferredoxin was converted to the 3Fe ferredoxin by exposure to air during aerobic purification. Therefore, it can be proposed that *T. profundus* ferredoxin exists in cells as the 4Fe ferredoxin and is degraded to the 3Fe ferredoxin during aerobic purification because of its oxygen sensitivity. The degradation of the 4Fe ferredoxin to the 3Fe ferredoxin is supported by the finding that both ferredoxins have the same amino acid sequence from the N-terminus to the 26th residue.

In addition, the aerobically-purified *T. profundus* ferredoxin was converted back to the 4Fe ferredoxin by the addition of ferrous ions under reducing conditions (Fig. 4e). The

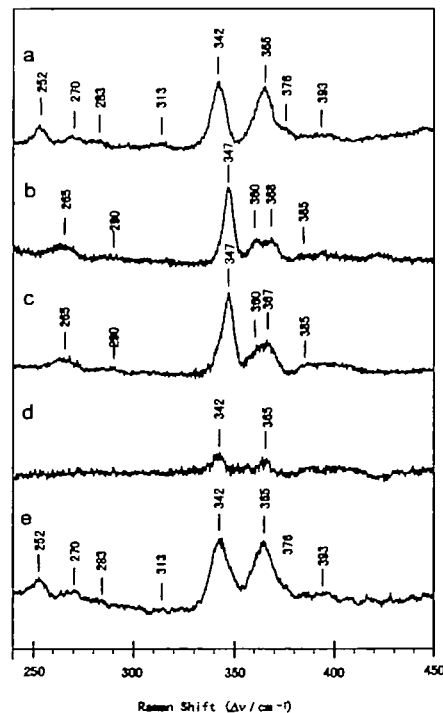


Fig 4. Resonance Raman spectra of *T. profundus* ferredoxins at 77 K. Excitation by Ar⁺ laser (457.9 nm) was used with a spectral band width of 6 cm⁻¹. (a) The anaerobically-purified ferredoxin exposed briefly to air. Ten scans were averaged. (b) Ferredoxin treated with a five-fold molar excess of ferricyanide (Ten scans). (c) Aerobically-purified ferredoxin (twelve scans). (d) Difference spectrum (spectrum 3c minus 3b). (e) Anaerobically-purified ferredoxin reconstituted with ferrous ion under reducing conditions. The sample concentrations were 5–8 mM in 10 mM Tris-HCl (pH 8.0).

reconstitution reaction was fast compared to the slow degradation to the [3Fe-4S] cluster. Such fast ferrous ion incorporation in the reconstitution reaction resembles that of *P. furiosus* ferredoxin, which contains the Fe-S cluster binding motif CXXDXXCXXXCP (9).

Comparison of *T. profundus* Ferredoxin with *P. furiosus* Ferredoxin—Most ferredoxins that contain the Fe-S binding motif, CXXDXXCXXXCP, in the N-terminal region have been shown to be oxygen-sensitive to a greater or lesser degree. It has been reported that *P. furiosus* 4Fe ferredoxin is partially degraded to 3Fe ferredoxin during aerobic purification and is not degraded to the 3Fe ferredoxin at all upon exposure to air if it had been purified as the 4Fe ferredoxin under anaerobic conditions (9). In contrast, ferredoxin containing mainly the 3Fe cluster is purified from *T. profundus* under aerobic conditions. These results suggest that *T. profundus* ferredoxin is more oxygen-sensitive than *P. furiosus* 4Fe ferredoxin. The amino acid sequence of the N-terminal half of *T. profundus* ferredoxin is similar to that of *P. furiosus* ferredoxin (Fig. 1); the sequences are the same from the N-terminus to 27th residue, except for the 5th amino acid (Thr or Ser). However, 41% of the sequence from the 28th residue to the C-terminus are the same, including the cysteine residue at position 52, which is a

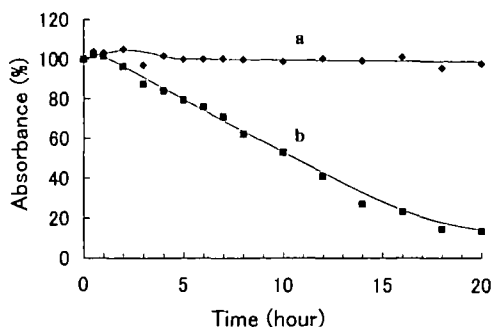


Fig 5. Thermal stability of *T. profundus* ferredoxins. The anaerobically-purified ferredoxin (a) and aerobically-purified ferredoxin (b) were both incubated at 100°C in 50 mM Tris-HCl (pH 8.0)/2 mM DTT under an Ar atmosphere and the absorbance changes at 440 nm were monitored

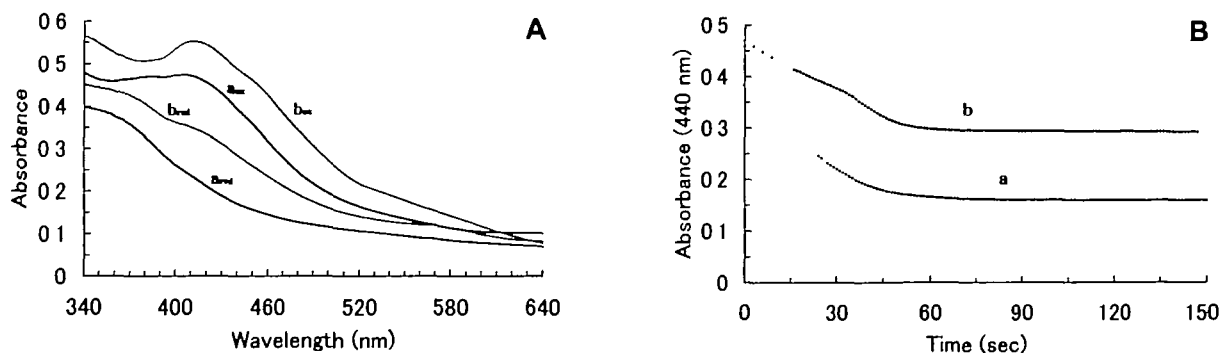


Fig 6 Biological activities of *T. profundus* ferredoxins. (A) UV-visible absorption spectra of *T. profundus* ferredoxin before and after incubation at 80°C with *T. profundus* POR and its substrates (CoASH and pyruvate). The spectra were measured at 25°C. a_{ox} is the anaerobically-purified ferredoxin exposed briefly to air; a_{red} is the substrate-reduced anaerobically-purified ferredoxin; b_{ox} is the aerobically-purified ferredoxin; b_{red} is the substrate-reduced aerobically-purified fer-

ligand to the Fe-S cluster. Therefore, the difference in the oxygen sensitivity of these two proteins can be attributed to some non-identical, non-coordinated amino acid residue(s) in the C-terminal half. The contribution of some amino acids that are not ligands for the Fe-S cluster but are located close to the Fe-S cluster to the oxygen sensitivity has been suggested in the case of the 2Fe ferredoxin from *Anabaena variabilis* (29). In addition, the mutant protein of *Azotobacter vinelandii* ferredoxin I, whose second normal Fe-S binding motif is converted to a 39 CXXDXXCXXXCP motif, has been found to be stable to oxygen attack (28). These results suggest that the region surrounding the motif, but not the motif sequence itself, is important for determining the oxygen sensitivity of ferredoxins.

Thermal Stability—The thermal stabilities of the anaerobically- and aerobically-purified ferredoxins under anaerobic conditions were examined by following the absorbance change during incubation. The results in Fig. 5 show that the absorbance at 440 nm of the anaerobically-purified *T. profundus* 4Fe ferredoxin did not decrease but increased slightly during the initial several hours. The reason for the slight absorbance increase is not clear. After 5 h until 20 h, the absorbance remained almost constant, indicating that the ferredoxin is extremely thermostable. In addition, the aerobically-purified ferredoxin was also found to be thermostable. There was also a slight increase in the absorbance, although it was less stable at 100°C compared to the anaerobically-purified ferredoxin; the half-life of the aerobically-purified ferredoxin under an anaerobic atmosphere was 10 h at 100°C (Fig 5). After 10 h of incubation at 100°C, we measured the resonance Raman spectrum of the 3Fe ferredoxin to examine the formation of 2Fe ferredoxin during the degradation to apoferredoxin. The spectrum obtained shows only the presence of 3Fe ferredoxin. The results indicate that the 3Fe ferredoxin is degraded to apoferredoxin(s) without the formation of 2Fe ferredoxin. The thermostability of the *T. profundus* 4Fe ferredoxin is comparable to those of such ferredoxins as the *T. maritima* 4Fe ferredoxin and the *P. furiosus* 4Fe ferredoxin (30–32).

Biological Activity—The biological activities of both the anaerobically- and aerobically-purified *T. profundus* ferredoxins were examined for their abilities to accept electrons

ferredoxin (B) Reduction rates of the two ferredoxins by *T. profundus* POR and its substrates as measured by following the absorbance change at 440 nm at 80°C under anaerobic conditions: a: anaerobically-purified ferredoxin, b: aerobically-purified ferredoxin. Dotted lines are the possible reduced curves at the beginning of the reaction on the basis of the original absorbance of each sample.

from the enzyme, *T. profundus* pyruvate-ferredoxin oxidoreductase (POR). Incubation with *T. profundus* POR and its substrates at 80°C caused absorbance decreases in the visible region of both *T. profundus* ferredoxins (Fig 6A). The time courses of the absorbance decreases at 440 nm for the two ferredoxins as shown in Fig. 6B indicate that both were reduced at similar rates. In the fully-reduced state, 58 ± 6% of the absorbance at 440 nm was lost in the anaerobically-purified *T. profundus* ferredoxin, while 36 ± 4% was lost in the case of the aerobically-purified ferredoxin. These results indicate that both ferredoxin preparations accept electrons from *T. profundus* POR. It is probable that the 4Fe ferredoxin functions as a native electron acceptor because the purified *T. profundus* ferredoxin under anaerobic conditions is the 4Fe-type. The addition of excess sodium dithionite to the POR-reduced ferredoxins resulted in a slight further absorbance decrease in the visible region of both ferredoxins. In addition, exposure of the POR-reduced ferredoxin to the air resulted in almost a complete recovery (>95%) of the absorbance in the visible region.

On the basis of X-ray crystallographic analysis (6), the removable Fe atom, whose external ligand is aspartate, in the [4Fe-4S] cluster of *P. furiosus* ferredoxin has been found to be located at the gate of its electron transfer from *P. furiosus* formaldehyde-ferredoxin oxidoreductase (FOR). From the amino acid sequence similarity, it is highly probable that *T. profundus* 4Fe ferredoxin has a similar three-dimensional structure to *P. furiosus* 4Fe ferredoxin. Therefore, it is possible to postulate that the *T. profundus* 4Fe ferredoxin has a removable Fe atom in the Fe-S cluster as in the *P. furiosus* 4Fe ferredoxin. Accordingly, it seems reasonable to assume that the *T. profundus* 4Fe ferredoxin will lose its electron acceptor ability upon release of the Fe atom from the [4Fe-4S] cluster due to oxidative damage. Contrary to the above assumption, the electron transferred to *T. profundus* POR from pyruvate was transferred further to the *T. profundus* 3Fe ferredoxin, as well as to the 4Fe ferredoxin. Therefore, we consider two possible explanations for this phenomenon: (i) the electron transfer path from *T. profundus* POR to ferredoxin is different from that from *P. furiosus* FOR to the 4Fe ferredoxin, and/or (ii) the structure of the *T. profundus* 3Fe ferredoxin, especially the structure of the [3Fe-4S] core produced by the deletion of one Fe atom, is different from the *T. profundus* 4Fe core structure. Further structural studies will help to clarify the mechanism of the electron transfer from the reduced POR to the ferredoxins.

The authors wish to thank Dr E. Horn for correcting the manuscript, and also Mrs. Tadanori Fueki, Yukio Amagai, and Koichi Tanimizu for technical assistance.

REFERENCES

- Fukuyama, K., Y. Nagahara, Tsukihara, T., and Katsube, Y., Hase, T., and Matsubara, H. (1988) Tertiary structure of *Bacillus thermoproteolyticus* [4Fe-4S] ferredoxin Evolutionary implications for bacterial ferredoxins. *J. Mol. Biol.* **199**, 183–193
- Fukuyama, K., Matsubara, H., Tsukihara, T., and Katsube, Y. (1989) Structure of [4Fe-4S] ferredoxin from *Bacillus thermoproteolyticus* at 2.3 Å resolution. *J. Mol. Biol.* **210**, 383–398
- Kissinger, C.R., Sieker, L.C., Adman, E.T., and Jensen, L.H. (1991) Refined crystal structure of ferredoxin II from *Desulfovibrio gigas* at 1.7 Å. *J. Mol. Biol.* **219**, 693–715
- Sery, A., Housett, D., Serre, L., Binicel, J., Hatchkian, C., Frey, M., and Roth, M. (1994) Crystal structure of the ferredoxin I from *Desulfovibrio africanus* at 2.3 Å resolution. *Biochemistry* **33**, 15408–15417
- Macedo-Ribeiro, A., Darimont, B., Sterner, R., and Huber, H. (1996) Small structural changes account for the high thermostability of [4Fe-4S] ferredoxin from the hyperthermophilic bacterium *Thermotoga maritima*. *Structure*, **4**, 1291–1301
- Hu, Y., Faham, S., Roy, R., Adams, M.W.W., and Rees, D.C. (1999) Formaldehyde ferredoxin oxidoreductase from *Pyrococcus furiosus*: The 1.85 Å resolution crystal structure and its mechanistic implications. *J. Mol. Biol.* **286**, 899–914
- Bruschi, M. and Guerlesquin, F. (1988) Structure, function and evolution of bacterial ferredoxins. *FEMS Microbiol. Rev.* **54**, 155–176
- Calzolari, L., Gorst, C.M., Zhou, Z.H., Teng, Q., Adams, M.W.W., and La Mar, G.N. (1995) ¹H-NMR investigation of the electronic and molecular structure of the four-iron cluster ferredoxin from the hyperthermophile *Pyrococcus furiosus*. Identification of Asp 14 as a cluster ligand in each of the four redox states. *Biochemistry* **34**, 11373–11384
- Conover, R.C., Kowal, A.T., Fu, W., Park, L.-B., Aono, S., Adams, M.W.W., and Johnson, M.K. (1990) Spectroscopic characterization of the novel iron-sulfur cluster in *Pyrococcus furiosus* ferredoxin. *J. Biol. Chem.* **265**, 8533–8541
- Kobayashi, T., Kwak, Y.S., Akiba, T., Kudo, T., and K. Horikoshi (1994) *Thermococcus profundus* sp. nov., A new hyperthermophilic archaeon isolated from a deep-sea hydrothermal vent. *System Appl. Microbiol.* **17**, 232–236
- Weber, K. and Osborn M. (1969) The reliability of molecular weight determination by dodecylsulfate-polyacrylamide gel electrophoresis. *J. Biol. Chem.* **244**, 4406–4412
- Davis B.J. (1964) Disc electrophoresis-II Method and application to human serum proteins. *Ann NY Acad Sci.* **121**, 404–427
- Lowry, O.H., Rosebrough, N.J., Farr, A.L., and Randall R.J. (1951) Protein measurement with the Folin phenol reagent. *J. Biol. Chem.* **193**, 265–275
- Masse, V. (1957) Studies of succinic dehydrogenase. VII. Valency state of the iron in beef heart succinic dehydrogenase. *J. Biol. Chem.* **229**, 763–770
- King, T.E. and Morris, R.O. (1967) Determination of acid-labile sulfide and sulfhydryl group in *Methods in Enzymology*, Vol. 10, pp. 634–637, Academic Press, New York
- Heltzel, A., Smith, E.T., Zhou, Z.H., Blamey, J.M., and Adams M.W.W. (1995) Cloning, expression, and molecular characterization of the gene encoding an extremely thermostable [4Fe-4S] ferredoxin from the hyperthermophilic archaeon *Pyrococcus furiosus*. *J. Bacteriol.* **176**, 4790–4793
- Imai, T., Matsumoto, T., Ohta, S., Ohmori, D., Suzuki, K., Tanaka, J., Tsukioka, M., and J. Tobarri (1983) Isolation and characterization of a ferredoxin from *Mycobacterium smegmatis*. *Biochim Biophys. Acta* **743**, 91–97
- Imai, T., Saito, H., Tobarri, J., Ohmori, D., and Suzuki, K. (1984) Resonance Raman spectroscopic evidence for the presence of 4Fe and 3Fe centers in *Pseudomonas ovalis* ferredoxin and *Mycobacterium smegmatis* ferredoxin. *FEBS Lett.* **165**, 227–230
- Imai, T., Kamata, K., Saito, H., and Urushiyama, A. (1995) Effect of hexacyano-ferrate (III) on *Mycobacterium smegmatis* ferredoxin. Further evidence for formation of a 6Fe(2x[3Fe-4S]) ferredoxin. *Bull. Chem. Soc. Jpn.* **68**, 2923–2930
- Blamey, J.M. and Adams, M.W.W. (1993) Purification and characterization of pyruvate-ferredoxin oxidoreductase from the hyperthermophilic archaeon *Pyrococcus furiosus*. *Biochim. Biophys. Acta*, **1161**, 1008–1016
- Siddiqui, M.A., Fujiwara, S., Takagi, M., and Imanaka, T. (1998) Phylogenetic analysis and effect of heat on conformational change of ferredoxin from hyperthermophilic archaeon *Pyrococcus* sp. KOD1. *J. Ferment. Bioeng.* **85**, 271–277
- Blamey, J.M., Mukund, S., and Adams, M.W.W. (1994) Properties of a thermostable 4Fe-ferredoxin from the hyperthermophilic bacterium *Thermotoga maritima*. *FEMS Microbiol. Lett.*

- 121, 165–170
- 23 Darimont B and Sterner R. (1994) Sequence, assembly and evolution of a primordial ferredoxin from *Thermotoga maritima*. *EMBO J* **13**, 1772–1781
- 24 Bruschi, M. and Couchoud, P. (1979) Amino acid sequence of *Desulfovibrio gigas* ferredoxin, revision. *Biochem. Biophys. Res. Commun* **91**, 623–628
- 25 Davy, S.L., Breton, J., Osborne, M., Thomson, A.J., Thurgood, A.G.P., Lian, L.-Y., Petillot, Y., Hatchikian, C., and Moore, G.R. (1994) MCD and ¹H NMR spectroscopic studies of *Desulfovibrio africanus* ferredoxin I revised amino acid sequence and identification of secondary structure. *Biochim Biophys. Acta* **1209**, 33–39
- 26 Teng, Q., Zhou, Z.H., Smith, E.T., Busse, S.C., Howard, J.B., Adams, M.W.W., and La Mar, G.N. (1994) Solution ¹H-NMR determination of secondary structure for the three-ion form of ferredoxin from the hyperthermophilic archaeon *Pyrococcus furiosus*. *Biochemistry* **33**, 6316–6326
- 27 Johnson, M.K., Czernuszewicz, R.S., Spiro, T.G., Fee, J.A., and Sweeney, W. (1983) Resonance Raman spectroscopic evidence for a common [3Fe-4S] structure among proteins containing three-iron centers. *J Am Chem. Soc.* **105**, 6671–6678
28. Jung, Y-S, Bonagura, C.A., Tilly, G.J., Gao-Sheridann, H.S., Armstrong, F.A., Stout, C.D., and Burgess, B.K. (2000) Structure of C42D *Azotobacter vinelandii* FdI A Cys-X-X-Asp-X-X-Cys motif ligates an air-stable [4Fe-4S]²⁺ cluster. *J Biol Chem.* **275**, 36974–36983
- 29 Singh, B.B., Curdt, I., Jakobs, C., Shomburg, D., Bisen, P.S., and Bohme, H. (1999) Identification of amino acids responsible for the oxygen sensitivity of ferredoxins from *Anabaena variabilis* using site-directed mutagenesis. *Biochim Biophys. Acta* **1412**, 288–294
- 30 Pfeil, W., Gesierich, U., Kleemann, B.R., and Sterner, R. (1997) Ferredoxin from the hyperthermophile *Thermotoga maritima* is stable beyond the boiling point of water. *J. Mol. Biol.* **272**, 591–596
31. Aono, S., Bryant, F.O., and Adams M.W.W. (1989) A novel and remarkably thermostable ferredoxin from the hyperthermophilic archaeobacterium *Pyrococcus furiosus*. *J Bacteriol* **171**, 3433–3439
- 32 Klump, H.H., Robb, F.T., and Adams, M.W.W. (1994) Life in the pressure cooker: The thermal unfolding of proteins from hyperthermophiles. *Pure. Appl. Chem.* **66**, 485–489